A reappraisal of the phylogeny of the Megatheria (Mammalia: Tardigrada), with an emphasis on the relationships of the Thalassocninae, the marine sloths

Eli Amson, Christian de Muizon, Timothy J. Gaudin

A reappraisal of the phylogeny of the Megatheria (Mammalia: Tardigrada), with an emphasis on the relationships of the Thalassocninae, the marine sloths.

Eli Amson[1,2,3]*, Christian de Muizon[1], and Timothy J. Gaudin[4].

[1], Centre de Recherche sur la Paléobiodiversité et les Paléoenvironnements (CR2P: CNRS, MNHN, UPMC-Paris 06; Sorbonne Universités), Muséum national d'Histoire naturelle, CP38, 57 rue Cuvier, 75005 Paris, France.

[2], Paläontologisches Institut und Museum, Universität Zürich, Karl Schmid-Strasse 4, CH-8006 Zürich, Switzerland.

[3], Humboldt-Universität, AG Morphologie und Formengeschichte & Institut für Biologie, Philippstraße 12/13, Haus 2, D-10115, Berlin, Germany.

[4], Department of Biological & Environmental Sciences, University of Tennessee at Chattanooga, 615 McCallie Ave., Chattanooga, TN 37403-2598, USA.

*, corresponding author: eli.amson@edu.mnhn.fr.

Running Title: Phylogeny of the Megatheria.

Abstract

The Thalassocninae is a monogeneric subfamily of five species of Neogene sloths. Until now, *Thalassocnus* has been considered as belonging to the Nothrotheriidae, a family of megatherian "ground sloths" of intermediate body size. However, no previous phylogenetic analysis has questioned such a familial attribution. Here we perform an extensive analysis including the required taxonomic sampling for such an attribution and characters from the whole skeleton. We found that *Thalassocnus* indeed belongs to Megatheria, but is clustered among Megatheriidae, the family that includes the large-size *Megatherium*. Moreover, the relationships among the five species of *Thalassocnus* are congruent with their respective stratigraphic positions, which allows the recognition of numerous morphoclines that document the adaptation of this sloth to the marine environment.

Keywords: Megatheria - Megatheriidae - Nothrotheriidae - Phylogeny - Postcranial skeleton - Tardigrada - *Thalassocnus* - Xenarthra.

Introduction

The "ground sloth" *Megatherium americanum* Cuvier, 1796 is an iconic taxon for several reasons, the most obvious being its large body mass (estimated to be around 4, 000 kg; Fariña, Vizcaíno, & Bargo, 1998). But its study by renowned early authors such as Georges Cuvier (Cuvier, 1804) and Richard Owen (Owen, 1861), as well as its recent extinction [during the Pleistocene–Holocene transition; Pujos *et al.* (2013)] have also contributed to its fame. There is also the fact that *M. americanum* differs so dramatically in terms of body size and (purported) ecology, from its closest extant relatives, the "tree sloths." *M. americanum* is considered to be a terrestrial browser (more precisely a selective feeder; Bargo & Vizcaíno, 2008) and more agile than extant "tree sloths" (probably less 'sluggish'; Billet *et al.*, 2013). *M. americanum* is the type species of *Megatherium*, the type genus of the family Megatheriidae. According to Gaudin (2004), this family forms a larger clade Megatheria, with the family Nothrotheriidae and a few other genera. There are three additional tardigradan families - the Megalonychidae (which forms with the Megatheria the Megatherioidea), the Mylodontidae (included in the Eutardigrada along with the Megatherioidea) and the Bradypodidae (which only includes the extant species of *Bradypus*; Gaudin, 2004).

Thalassocnus is unique among sloths (and more generally among xenarthrans) because it has been interpreted as adapted to the aquatic realm (Muizon & McDonald, 1995; Amson *et al.*, 2014, 2015a,b,c). Most of the *Thalassocnus* specimens come from the Pisco Formation (Peru), which comprises a rich marine vertebrate fauna (Muizon & DeVries, 1985; Bianucci *et al.*, 2015). A few isolated specimens were also recovered from the Bahía Inglesa Formation (Canto *et al.*, 2008; Pyenson *et al.*, 2014) and from an undescribed locality at a latitude of 30° South on the Chilean coast (Saleta de los Arcos

and F. Amaro Mourgues, pers. com.). *Thalassocnus* is comprised of five Neogene species that together form the monogeneric subfamily Thalassocninae (Muizon *et al.*, 2004a). *Thalassocnus* was initially placed among the Nothrotheriidae (considered a subfamily at that time) with the understanding that the latter taxon was more closely related to Megalonychidae than to Megatheriidae (Muizon & McDonald, 1995). Whereas Gaudin (2004) considered the Nothrotheriidae to be more closely related to Megatheriidae than to Megalonychidae, *Thalassocnus* was not included in his study. Phylogenetic analyses including *Thalassocnus* (Muizon & McDonald, 1995; McDonald & Muizon, 2002; Muizon *et al.*, 2003; De Iuliis, Gaudin, & Vicars, 2011) did not question its inclusion in the Nothrotheriidae (or Nothrotheriinae), since the ingroups in each of these studies only included terminal taxa pertaining to this clade. It must be noted, however, that decades before the formal description of the first species, *Thalassocnus* material was first attributed to an undescribed megatheriid, possibly a planopsine (one of the two megatheriid subfamilies classically recognized), mainly based on the morphology of the astragalus and femur (Hoffstetter, 1968).

The work of Gaudin (2004) can be regarded as the most comprehensive phylogeny of the Tardigrada published to date. With the addition of mandibular, dental, and other cranial characters to the auditory region traits used in Gaudin (1995), the data matrix of Gaudin (2004) reaches a total of 286 characters. While taking into consideration the cranial, mandibular and dental characters of previous analyses (for instance, Engelmann, 1985; Patterson *et al.*, 1992), this synthetic work did not include postcranial characters. Even though De Iuliis (1994) did not perform a cladistic analysis *per se*, his work focused on the relationships among megatheriines, nothrotheriines and planopsines, and postcranial characters were discussed. Pujos *et al.* (2007) performed an analysis that included 17 postcranial characters and sampled all the tardigradan

families, but they considered their analysis preliminary, and did not include *Thalassocnus*.

As the basis of our investigation, a data matrix has been built using postcranial characters, as well as the characters of Gaudin (1995, 2004). The present analysis incorporates dental and osteological characters of the whole skeleton and comprises an appropriate taxonomic sample to test hypotheses regarding the familial attribution of *Thalassocnus* within sloths. Additionally, the present study is the first that includes all species of *Thalassocnus* as terminal taxa, which allows us to test previously hypothesized intrageneric relationships..

Abbreviations

Institutions: **FMNH**, Field Museum of Natural History, Chicago, Illinois, USA; **LACM**, Natural History Museum of Los Angeles County, Los Angeles, California, USA; **MCL**, Museu de Ciencias Naturais da Pontifícia Universidade Católica de Minas Gerais, Belo Horizonte, Minas Gerais, Brazil; **MNHN**, Muséum national d'Histoire naturelle, Paris, France; **NHMUK**, Natural History Museum, London, United Kingdom.

Other: **CI**, Consistency index; **ch.**, character; **MPT**, most parsimonious tree; **OTU**, operational taxonomic unit; **RI**, retention index; **SALMA**, South American Land Mammal Age.

Material and methods

Data matrix

A data matrix of 347 osteological characters was generated. The 54 postcranial characters are either newly described or taken (and modified in some cases) from

previous analyses (Muizon *et al.*, 2003; Pujos *et al.*, 2007; De Iuliis *et al.*, 2011). A detailed description of these characters with their states can be found below. Seven cranial and mandibular characters of particular relevance regarding the relationships among the species of *Thalassocnus* were taken from Muizon *et al.* (2003), and are also described below. The 286 dental, mandibular, and cranial characters (including those of the auditory region) of Gaudin (1995, 2004) were all added to the matrix, without any modification from the initial coding.

All the Megatheria from the analysis of Gaudin (2004), namely *Nothrotherium*, *Nothrotheriops*, *Mionothropus* (referred to as *Nothropus* in Gaudin, 2004), *Pronothrotherium*, *Eremotherium* (the species *E. laurillardi* Lund, 1842 was coded), *Megatherium* (the species *M. americanum* was coded), and *Planops* (for the postcranial characters, only *P. martini* Hoffstetter, 1961 was used), were included as OTUs in the matrix. The closely related *Analcimorphus* and *Hapalops* [two taxa from the Santacrucian SALMA, early Miocene; Scott (1903-1904)], and the megalonychids *Megalonyx* (a well-known Plio-Pleistocene taxon) and *Eucholoeops* (the oldest well-known megalonychid) were also added, since *Thalassocnus*, as a "nothrotheriid," was once considered closely related to megalonychids (Muizon & McDonald, 1995), and *Analcimorphus* and *Hapalops* were allied as successive sister-taxa to either Megatheria or Megalonychidae in Gaudin (2004). Each of the species of *Thalassocnus* was coded as a terminal taxon, based on specimens from the Pisco Formation. These are *T. antiquus* Muizon *et al.*, 2003 (Aguada de Lomas horizon, *ca.* 8 Myr), *T. natans* Muizon & McDonald (Montemar horizon, *ca.* 7 Myr), 1995, *T. littoralis* McDonald & Muizon, 2002 (SAS horizon, *ca.* 6 Myr), *T. carolomartini* McDonald & Muizon, 2002 (Sacaco horizon, *ca.* 5 Myr), and *T. yaucensis* Muizon *et al.*, 2004 (< *ca.* 5 Myr, probably early Pliocene). The Santacrucian sloth genera *Schismotherium* and *Pelecyodon*, the sister taxa of all other Megatherioidea [either one,

the other, or a clade that comprises both of them, depending on the MPTs of (2004)] were included as well. Finally, in order to root the phylogenetic tree, we used a first outgroup comprising three mylodontids for which fairly complete specimens are known [the Santacrucian taxon *Nematherium*, and the well-known Plio-Pleistocene genera from the two main mylodontid subfamilies, *Glossotherium* (Mylodontinae) and *Catonyx* (Scelidotheriinae)]. As a second outgroup, the extant three-toed sloth *Bradypus*, sister group of the Eutardigrada (*sensu* Gaudin 2004), was used. While we recognized mylodontids as a first outgroup because we considered unlikely a priori that *Thalassocnus* would ally with them, the presence of a second outgroup allows testing the monophyly of the ingroup (here the Megatherioidea), and hence the possibility that *Thalassocnus* is more closely related to mylodontids. This brings to 22 the number of terminal taxa in the data matrix (Table 1). The whole character matrix, including the coding of craniomandibular and dental characters of Gaudin (2004) and Muizon *et al.* (2003), is provided in Appendix 1 as a NEXUS file. The correspondence between the numbering system used here and those of Gaudin (1995, 2004) is given in Appendix 1. The source of the coding for each taxon can be found in Table 2, and includes both information from the literature and direct observations of specimens.

Description of the characters and their states.

Refer to Gaudin (1995, 2004) regarding his characters (here numbered 62-347, see Appendix 1). In the following description, and in the case of characters in which the states differ among the *Thalassocnus* species, the reader is invited to refer to previous works that describe the anatomy of the forelimb (Amson *et al.*, 2015a), hind limb (Amson *et al.*, 2015b), axial postcranium (Amson *et al.*, 2015c), and skull (McDonald & Muizon, 2002; Muizon *et al.*, 2003, 2004a) within this genus.

Forelimb

1. Humerus, ratio of greatest proximodistal length to mediolateral width of distal articular surface ratio: 0) high (greater than 4); 1) intermediate (between 3 and 4); 2) low (lower than 3). Ordered; see Appendix 3 for ratio values.

2. Humerus, brachiocephalicus crest: 0) absent or weakly developed (Fig. 1A, B, D); 1) well developed (Fig. 1C). See also Amson *et al.* (2015a: fig. 5).

3. Humerus, medial epicondyle: 0) angular and positioned proximally (Fig. 1A, B); 1) rounded and positioned distally (Fig. 1C, D). [Modified from De Iuliis *et al.* (2011), chs 40, 41]

4. Humerus, entepicondylar foramen: 0) present (Fig. 1A-C); 1) absent (Fig. 1D). [From Pujos (2002), ch. 20; Pujos *et al.* (2007), ch. 27]

5. Radius, development of pronator ridge on proximal fourth of diaphysis: 0) absent; 1) weak; 2) intermediate; 3) strong. See also Amson *et al.* (2015a: fig. 13).
Ordered.

6. Radius, bicipital tuberosity orientation: 0) projecting mainly posteriorly; 1) projecting mainly medially. [Modified from De Iuliis *et al.* (2011), ch. 44].

7. Radius, shape of extensor carpi radialis groove in lateral view: 0) strongly asymmetrical anteroposteriorly, not elongated anteroposteriorly and deep proximally; 1) weakly asymmetrical anteroposteriorly, weakly elongated anteroposteriorly and deep proximally (Fig. 2C); 2) symmetrical anteroposteriorly, strongly elongated anteroposteriorly and shallow proximally. Ordered; coded as not applicable if the groove is incipiently developed (Fig. 2A, B, D). See also Amson *et al.* (2015a: fig. 13).

8. Radius, extension of laterodistal process: 0) weak, proximal to level of styloid process (Fig. 2A, B); 1) strong, almost at the level or reaching level of styloid process (Fig. 2C, D).

9. Scaphoid, laterodistal corner in dorsal view: 0) not elongated, wedge-shaped (Fig. 3A-C); 1) elongated, quadrangular in outline [see Paula Couto (1974: fig. 1)]. [Modified from De Iuliis *et al.* (2011), ch. 51]

10. Lunar, general proportions (ratio of mediolateral width to proximodistal length): 0) longer than wide (ratio<1; Fig. 4A, B); 1) wider than long (ratio>1; Fig. 4C, D). See Appendix 3 for ratio values.

11. Lunar, distal extension of facet for radius on dorsal side: 0) reaches distal edge of the bone (Fig. 4B, C); 1) reaches only the midlength of the bone (Fig. 4A, D).

12. Lunar, contact with unciform: 0) absent (Fig. 3B); 1) present (Fig. 3A, C).

13. Cuneiform, proximal articular facet: 0) well developed mediolaterally (Fig. 3A, B); 1) reduced laterally (restricted to the mediodorsal corner of the proximal surface) or absent (Fig. 3C).

14. Cuneiform, mediodistal extension in dorsal view: 0) weak (Fig. 3A, C); 1), strong mediodistal process, tapering distally (Fig. 3B). See also Amson *et al.* (2015a: fig. 24). [Modified from De Iuliis *et al.* (2011), ch. 52]

15. Cuneiform, facet for Mc V: 0) absent, and no fossa *in situ*; 1) present; 2) absent, and fossa *in situ*. See Amson *et al.* (2015a: fig. 24). Ordered.

16. Magnum, contact with Mc II: 0) absent or minute (Fig. 3B); 1) well developed, thanks to the proximolateral process of Mc II that overlaps Mc III proximally (Fig. 3A, C). Coded as not applicable in *Bradypus* because the magnum is fused to the trapezoid.

17. Metacarpals II, III, and IV, facets of contact with adjacent metacarpals: 0) weakly extended distally (the metacarpals are hence widely diverging distally; Fig. 3B); 1) well extended distally (the metacarpals are roughly parallel or only slightly diverging; Fig. 3A, C). Coded as not applicable in *Glossotherium* because of the strong shortening of the metacarpus.

18. Trapezium-Mc I complex (MCC) reduction, ratio of proximodistal length to DP depth: 0) weak, shaft well developed (ratio > 3); 1) intermediate, shaft almost absent (2 < ratio < 3; Fig. 3A); 2) whole complex vestigial (ratio around 1.5 or below; Fig. 3C). Ordered; see Appendix 3 for ratio values. Coded as not applicable when the complex is absent.

19. Manus, digit I, number of phalanges: 0) 2 (proximal surface of ungual trochleated; Fig. 3B); 1) 1 (Fig. 3A); 2) 0 (Fig. 3C).

20. Mc II, proximodistal length to dorsopalmar depth ratio: 0) Mc II elongate (ratio > 3.7; Fig. 3B); 1) Mc II intermediate (3.7 > ratio > 3; Fig. 3A, C); 2) Mc II stout (ratio < 3); see Appendix 3 for ratio values.

21. Manus, digit II, ungual phalanx, shape of cross-section of ungual process: 0) triangular; 1) semicircular (Fig. 9); 2) dorsopalmarly flattened. [Modified from McDonald & Muizon (2002), ch. 28; Muizon *et al.* (2003), ch. 30; De Iuliis *et al.* (2011), ch. 55].

22. Manus, digit III, proximal and intermediate phalanges: 0) free (Fig. 3B); 1) coossified (Fig. 3A, C). [From McDonald and Muizon (2002), ch. 27; (Pujos, 2002) ch. 24; Pujos *et al.* (2007) ch. 29].

23. Manus, digit IV, ungual phalanx in dorsal view: 0) rectilinear (Fig. 3B, C); 1) curved medially (Fig. 3A).

24. Manus, digit V, ungual: 0) present; 1) absent (Fig. 3A-C).

Hindlimb

25. Pelvis, acetabulum, pubic cornu: 0) as elevated as ichiatic cornu, posterior end reaching or close to reaching posterior edge of acetabulum; 1) below level of ischiatic cornu, posterior end reaching half of anteroposterior length of acetabulum. See Amson *et al.* (2015b: fig. 45).

26. Femur, general proportions (ratio of proximodistal length to mediolateral width at midshaft): 0) mediolaterally wide (ratio below 5; Fig. 5A, B, D); 1) mediolaterally narrow (ratio over 5; Fig. 5C). See Appendix 3 for ratio values. [Modified from Pujos *et al.* (2007), ch. 33; De Iuliis *et al.* (2011), ch. 58]

27. Femur, fovea capitis, position on the articular surface: 0) entirely included within it (Fig. 5A, B); 1) partly excluded from it (located posterolaterally; Fig. 5C, D). Coded as not applicable because the fovea itself is absent in *Bradypus* and *Schismotherium* (Scott, 1903-1904).

28. Femur, third trochanter: 0) isolated, close to midshaft (Fig. 5A, B); 1) joins only the greater trochanter (Fig. 5C); 2) joins both the greater trochanter and the lateral condyle (hence the entire lateral side of the bone is marked by a crest; Fig. 5D); 3) joins lateral epicondyle only. Coded as not applicable in *Bradypus* because the third trochanter is absent. [Modified from McDonald & Muizon (2002), ch. 29; Pujos (2002), ch. 25; Pujos *et al.* (2007), ch. 31].

29. Femur, distal articular surfaces: 0) patellar trochlea and both condylar surfaces confluent (Fig. 6A-F); 1) patellar trochlea isolated or only abuts the condylar surfaces; (Fig. 6G); 2) patellar trochlea confluent with the lateral condylar surface only (Fig. 6H). [From McDonald & Muizon (2002), ch. 23; Pujos (2002), ch. 26; Pujos *et al.* (2007), ch. 32]

30. Femur, deep notch for medial cruciate (posterior) ligament: 0) absent (Fig. 6A, B, G, H); 1) present (Fig. 6C-F).

31. Femur, medial trochlear ridge (ratio of anterior extension of medial trochlear ridge beyond lateral trochlear ridge to lateral one to anteroposterior femoral depth at lateral trochlear ridge): 0) ratio>0.25 (Fig. 6A, F, G); 1) ratio<0.25 (Fig. 6B-E). Coded as not applicable in *Megatherium* and *Eremotherium* since there is no trochlear ridge *per se*, the

patellar surface being reduced and confluent with the lateral condyle. See Appendix 3 for ratio values except for *Analcimorphus* and *Eucholoeops* for which the medial trochlear ridge does not protrude at all anteriorly, hence having null ratios.

32. Patella, general shape in anterior view: 0) roughly quadrangular; 1) teardrop shape, due to distal tapering and well-developed apex.

33. Tibia, proximodistal length compared to that of femur: 0) short (roughly 70-80% of femur or lower); 1) long (roughly 90% of femur). See Appendix 3 for ratio values.

34. Tibia, proximal epiphysis, location of anterior border of lateral facet (in proximal view): 0) posterior to medial facet; 1) level with medial facet.

35. Astragalus, separation of distinct odontoid process: 0) poor, trochlea weakly modified; 1) intermediate, odontoid process well defined only on distal half of proximodistal length of tibial surface; 2) strong, odontoid process well defined along entire proximodistal length of tibial surface. Ordered. [Modified from (Pujos, 2002), ch. 27; Pujos *et al.* (2007), ch. 35]. Except for that of *Hapalops* and *Nematherium*, the astragali of the Santacrucian sloths were not observed by the authors. Although Toledo, Bargo, & Vizcaíno (2015) describe a poorly defined process in those taxa, except for *Analcimorphus* and *Pelecyodon*, for which it is apparently more defined, we prefer to leave their states as question marks.

36. Astragalus, angle formed by discoid and odontoid facets in distal view: 0) highly obtuse; 1) roughly at right angles to one another. Ordered. [Modified from Pujos (2002), ch. 29; Pujos *et al.* (2007), ch. 37]. *Megalonyx* and *Bradypus* are coded as not applicable because they lack a distinct odontoid facet.

37. Astragalus, orientation of navicular process: 0) faces laterodistally, navicular facet visible in fibular view; 1) faces directly distad, navicular facet not visible in fibular view; 2) faces mediodistally, navicular facet not visible in fibular view. Ordered.

38. Astragalus, position of process for navicular in distal view: 0) median, at the level of the junction of the odontoid and discoid facets (when these facets are present); 1) medial, at the level of the odontoid process (when this facet is present). [Modified from (Pujos, 2002) ch. 28; Pujos *et al.* (2007), ch. 36].

39. Astragalus, distance between ectal facet and lateral trochlea in fibular view: 0) long; 1) short. [From De Iuliis (1994)]

40. Calcaneum, tuber calcis, distal development of proximal processes: 0) weak (Fig. 7A, B); 1) strong (reaching at least the proximal third of the bone; Fig. 7C, D).

41. Calcaneum, sustentacular facet and cuboid surface: 0) separated; 1) widely confluent.

42. Calcaneum, oblique crest on plantar side: 0) absent; 1) present.

43. Mt I and digit I size: 0) metacarpal and digit strong (Mt I elongate, ungual present); 1) intermediate (Mt I short, ungual present; Fig. 8A); 2) metacarpal and digit weak (Mt I short or absent, ungual absent; Fig. 8B, C).

44. Pes, digit III, proximal and intermediate phalanges: 0) free; 1) coossified (Fig. 8A-C). [Modified from Pujos *et al.* (2007), ch. 41].

45. Mt IV, ratio of proximodistal length to mediolateral width: 0) Mt IV elongate (ratio around 5); 1) intermediate (ratio between 4 and 5); 2) Mt IV short (ratio lower than 4). Ordered. Coded as not applicable in *Bradypus* because the Mt IV is fused with the tarsus. See Appendix 3 for ratio values.

46. Mt IV, facets for cuboid and Mt III: 0) isolated or barely in contact; 1) broadly contiguous. Coded as not applicable in *Bradypus* because distal tarsals and metatarsals are fused

47. Mt V, angle formed by facets for cuboid and Mt IV: 0) roughly right ; 1) obtuse (around 120°); 2) almost flat. Ordered. Coded as not applicable in *Bradypus* because the Mt V is vestigial.

48. Mt V, orientation of articular facets for the cuboid and Mt IV: 0) medial; 1) mediodorsal. Coded as not applicable in *Bradypus* because the Mt V is vestigial.

49. Mt V, lateral process: 0) well developed laterally; 1) weak or absent. Coded as not applicable in *Bradypus* because the Mt V is vestigial.

50. Metatarsals, position relative to one another when pes is articulated (and tibial facet of astragalus positioned dorsally): 0) metatarsals arrayed mediolaterally; 1) stacked partly dorsoventrally (Fig. 8B, C); 2) full dorsoventral stacking (Fig. 8A).

Axial postcranium

51. Number of thoracic vertebrae: 0) 18 or more; 1) less than 18. Coded as polymorphic in *Bradypus* (Gaudin, 1999).

52. Caudal inclination of spinous process (angle between its cranial edge and a dorsoventral axis) at mid-thoracic region (around T8): 0) weak ($\alpha \approx 50°$); 1) intermediate ($\alpha \approx 60°$); 2) strong ($\alpha \approx 70°$). Ordered. Coded as not applicable in *Bradypus* because of the reduction of the spinous processes

53. Hemal arches, shape of most cranial elements: 0), 'Y-shaped'; 1) 'X shaped'. Coded as not applicable in *Bradypus* because of the reduction of the caudal vertebrae.

54. Rib compactness (for a given section, the ratio of surface occupied by bone to the whole sectional area): 0) below 0.8; 1) between 0.8 and 0.9; 2) above 0.9. Ordered. [Data from Amson *et al.* (2014)]

Craniomandibular characters of particular relevance for *Thalassocnus*.

55. Ratio of maximum visible length of premaxilla to maximum length of skull (including the premaxilla), both in ventral view: 0) low, premaxilla short (ratio<0.20); 1) intermediate (0.20<ratio<0.23); 2) high, premaxilla elongate (ratio>0.23). Ordered. See Appendix 3 for ratio values. [Modified from Muizon *et al.* (2003), ch. 4].

56. Premaxillae, anterior processes widened at their anterior tip: 0) absent; 1) present.

57. Angulation formed by the narial opening in lateral view: 0) lateral narial margin forms either right or obtuse angle with dorsal edge of premaxilla; 1) lateral edge of the narial opening forms a smooth, continuous sigmoid curvature with dorsal edge of premaxilla. [Modified from Muizon *et al.* (2003), ch. 7]. Coded as not applicable in *Megalonyx* and *Bradypus* because the premaxilla is very reduced.

58. Attachment of base of jugal to skull: 0) dorsal to M2, or more anterior; 1) dorsal to M3. [Modified from Muizon *et al.* (2003), ch. 12]

59. Posterior margin of pterygoids thickened and expanded mediolaterally: 0) absent; 1) weak; 2) strong. Ordered [Modified from Muizon *et al.* (2003), ch. 16]

60. Shape of anterior margin of mandibular symphysis in dorsal view: 0) tapered and narrow; 1) transversely expanded and spatulate. [Modified from Muizon *et al.* (2003), ch. 23]

61. Internal trough of spout of mandible: 0) reaches anterior edge of spout; 1) does not reach anterior edge of spout. [Modified from Muizon *et al.* (2003), ch. 24]. Coded as not applicable in *Glossotherium* because there is no trough.

Analysis

We performed a heuristic search using PAUP 4.0b10 (Swofford, 2002) (monitoring for the absence of bugs, sometimes occurring in the apomorphy list of this version; personal observation of EA), with a random-addition sequence, 1000 replicates,

and with equally weighted character states. The branch support values were calculated by manually adding steps to the shortest tree.

Illustration of *Planops martini*'s ungual phalanx

In the original description of *Planops martini* Hoffstetter, 1961, the author mentions an ungual phalanx twice without figuring it. The first mention is in the description of the lot that corresponds to the holotype ("trois phalanges dont une unguéale"; [three phalanges, including one ungual]; Hoffstetter, 1961, p. 61). The second mention of the ungual phalanx, in the description itself, is written in the conditional tense, denoting the hesitation of the author regarding the attribution (Hoffstetter, 1961, p. 80). However, the author does mention the second digit of the manus. The description states that this phalanx is less compressed than in *Hapalops*, that the dorsal side is transversely rounded, the palmar side flattened, and that the ungual bears a weak proximodistal curvature. Since the publication of Hoffstetter (1961), the ungual phalanx of the second digit of the manus was described in an additional nothrotheriid, *Mionothropus* (De Iuliis *et al.*, 2011), and in *Thalassocnus* (Amson *et al.*, 2015a). It has already been emphasized that the semicircular cross-section of the ungual process of the second digit of the manus is a distinctive traits of nothrotheriids [McDonald & Muizon (2002), ch. 28; Muizon *et al.* (2003), ch. 30; De Iuliis *et al.* (2011), ch. 55] and of the early species of *Thalassocnus*, *T. antiquus* (the later species of the genus being characterized by a dorsopalmar flattening of this process; Amson *et al.*, 2015a), as this cross-sectional shape is not found in other digits or taxa. Since the ungual process of the ungual phalanx of the holotype of *Planops martini* features this distinctive cross-sectional shape, and hence strongly resembles those of nothrotheriids and of *T. antiquus*, we can today

confirm Hoffstetter's (1961) tentative attribution. Given the systematic importance of this phalanx (see below), an illustration is included herein (Fig. 9).

Results

The analysis resulted in a single MPT (Fig. 10). The tree has a length of 948 steps. Its CI is 0.47 and RI is 0.62. There are no internal branches with a null length (see table of linkages in Appendix 4). Due to the pruning of most megalonychids, mylodontids, and outgroups from the matrix of Gaudin (2004), 46 characters coming from the latter matrix became constant in the present analysis; 23 variable characters were parsimony-uninformative (see Appendix 1).

Interspecific relationships of *Thalassocnus*

The monophyly of the genus *Thalassocnus* is supported by 51 unambiguous synapomorphies (and up to 83 synapomorphies depending on the optimization, see table of linkages in Appendix **Erreur ! Source du renvoi introuvable.**), among which six are postcranial: pubic cornu of acetabulum below the level of the ischiatic cornu and with weak posterior extension (ch. 25(0=>1); non-homoplastic), slender femur (ch. 26(0=>1); Fig. 5A), teardrop-shaped patella (ch. 32(0=>1); non-homoplastic), stoutness of the Mt IV (ch. 45(2=>0); CI=2/5, RI=2/5), mediodorsal orientation of cuboid and Mt IV facets on Mt V (ch. 48(0=>1); non-homoplastic), and the acquisition of an intermediate (>60°) caudal inclination of the spinous processes of the mid-thoracic region (ch. 52(0=>1) ; CI=3/4, RI=2/3). Among the 45 unambiguous cranial synapomorphies, nine are non-homoplastic: trough of spout of mandible does not reach

anterior edge of spout (ch. 61(0=>1)), teeth implanted vertically (ch. 66(1=>0)), mandibular condyle convex medially and concave laterally in posterior view (ch. 116(2=>3)), nasal width increases anteriorly (ch.162 (1=>2)), presence of two lacrimal foramina (ch. 202(0=>1)), infraorbital foramen unexposed in ventral view (ch. 218(1=>0), parietal without distinct anteroventral process (ch. 240(1=>0)), occipital condyle roughly triangular but extended far medioventrally in posterior view (ch. 253(1=>2)), and presence of a glenoid posterior shelf (ch. 342(0=>1)) (see Appendix 5 for complete list of apomorphies).

The present analysis confirms the position of the earliest species, *T. antiquus* (*ca.* 8 Myr) as sister-group of the other species in the genus. Such a position was already suggested by Muizon *et al.* (2003) and Amson *et al.* (2015c). Furthermore, the relationships among the later species of the genus are also congruent with the stratigraphic position of each species, with *T. natans* (*ca.* 7 Myr) being sister-group of the three later species (forming the clade Th.1 in Fig. 10), and *T. littoralis* (*ca.* 6 Myr) being sister-group of the two later species (forming the clade Th.2 in Fig. 10), *T. carolomartini* (*ca.* 5 Myr) and *T. yaucensis* (< *ca.* 5 Myr; the two latter species form the clade Th.3 in Fig. 10). These relationships are supported by three (Th.1), seven (Th.2), and one (Th.3) unambiguous synapomorphy respectively (Appendix 4): Th.1 is defined by a well-developed brachiocephalicus crest (ch. 2(0=>1); CI= 1/2, RI=3/4), a lunar that is wider than long (ch. 10(0=>1); CI=1/2, RI=2/3), and a weakly developed medial trochlear ridge of the femur (ch. 31(0=>1); CI= 1/4, RI=2/5); Th.2 is defined by the absence of facet a for Mc V on the cuneiform (ch. 15(0=>1); CI=2/3, RI=1/2), the presence of a deep notch for medial cruciate ligament on the femur (ch. 30(0=>1); CI=1/2, RI=2/3), a Mt IV of intermediate stoutness (ch. 45(0=>1); CI=2/5, RI=2/5), a long premaxilla (ch.55(1=>2); CI=1/2, RI=3/4), lateral edge of narial opening forming a

smooth sigmoid curvature in lateral view (ch. 57 (0=>1); non-homoplastic), a spatulate mandibular symphysis (ch. 60(0=>1); CI=1/2, RI=2/3), and a relatively long preorbital region (ch. 146(1=>0); CI≈0.4, RI≈0.6); Th.3 is defined by a strong mediodistal process of the cuneiform (ch. 14(0=>1); CI=1/2, RI=1/2). Several of the characters supporting clades within *Thalassocnus* involve morphoclines extending from the earliest to the latest species, e.g., the development of pronator ridge of the radius (ch. 5(0=>1=>2=>3)), the caudal inclination of the spinous processes of the mid-thoracic region (ch. 52(1=>2=>3)), or bone compactness (ch. 54(0=>1=>2). For some of the continuously variable characters, the rather arbitrary discretisation of the states directly conditions the number of synapomorphies recognized for each clade within the genus. We view each of these clades as well supported, and the number of synapomorphies given here as the mere result of one example of character coding.

Thalassocnus within the Tardigrada

The present analysis is the first to place *Thalassocnus* (considered as such) among megatheriids. A Megatheriidae that includes *Thalassocnus*, is supported by nine unambiguous synapomorphies (and up to 36 depending on the optimization), among which four are postcranial: rounded and distally positioned medial epicondyle of the humerus (ch. 3(0=>1); CI=1/2, RI≈0.9; Fig. 1C, D), laterodistal process of radius extending far distally (ch. 8(0=>1); non-homoplastic; Fig. 2C, D), a strongly distinct odontoid process of the astragalus (ch. 35(1=>2); CI=2/5, RI=2/3), and sustentacular and cuboid facets of the calcaneum widely confluent (ch. 41(0=>1); CI=1/2, RI=4/5). The craniodental synapomorphies of the Megatheriidae are: an elongate condyloid process (ch. 112(2=>0); CI=2/5, RI=2/3), a plane of the condylar articular surface that changes mediolaterally (ch. 121(0=>1); CI=1/3; 2/3), an elongate symphysis (ch. 123

(2=>3); CI=2/3, RI≈0.9), moderately developed symphyseal spout (ch. 129 (1=>2); CI=2/5, RI=2/3), and the absence of clear demarcation between symphysis and horizontal ramus (ch. 130(0=>1); non-homoplastic). Furthermore, the Megatheriinae and *Thalassocnus* are united by 15 unambiguous synapomorphies (and up to 57 depending on the optimization), the postcranial ones are: short humerus (ch. 1(0=>1); CI=1/2, RI≈0.7), fovea capitis only partially included in the femoral head articular surface (ch. 27(0=>1); CI=0.5, RI≈0.8; Fig. 5C, D), anterior border of medial and lateral facets of the proximal tibia at same level (ch. 34(0=> 1); CI=1/2, RI≈0.9), right angle between the odontoid and discoid facets of the astragalus in distal view (ch. 36(0=>1); CI=1/3, RI=1/2), and strong development of the proximal processes of the tuber calcis (ch. 40(0=>1); CI=1/2, RI=0.9; Fig. 7C, D). For this last character, *Planops*, positioned in our results as the sister-taxon to all other included megatheriids, features an interesting condition (Fig. 7B). Because its lateroproximal process extends more distally than that of non-megatheriid megatherioids (Fig. 7A), it can be viewed as having an intermediate condition, when compared to those of other megatheriids (*Thalassocnus* included), in which this process and the medioproximal process are more developed distally (Fig. 7C, D). The megatheriines and *Thalassocnus* also share ten unambiguous craniodental apomorphies, among them: toothrow horizontal in lateral view (ch. 64 (2=>0); CI=1/2, RI=3/5), tympanic fused dorsally (ch. 265 (0=>1); CI=1/3, RI=3/4), and hemispherical glenoid (ch. 338 (0=>1); CI=0.5, RI=4/5).

Other relationships among Megatherioidea

While not the focus of the present study, some comments can be made regarding the other nodes of the tree produced by our analysis. As in previous phylogenetic analyses (Gaudin, 2004; Pujos *et al.*, 2007; and references therein), the Megatheria, a

clade comprising the megatheriids and the nothrotheriids, is recovered. While this clade was supported by only four unambiguous synapomorphies in Gaudin (2004), seven unambiguous synapomorphies are obtained here (and up to 31 depending on the optimization). Only two of those are postcranial synapomorphies. This could suggest that the inclusion of *Thalassocnus* itself in an analysis that comprises both families of Megatheria further substantiates the recognition of this clade, although the modification of the taxonomic sample when compared to the analysis of Gaudin (2004) cannot be ruled out as an alternative cause of the increase of unambiguous synapomorphies for the Megatheria. Concerning their postcranium, the Megatheria are defined by the medially projecting bicipital tuberosity of the radius (ch. 6(0=>1)), and the prominent anterior extension of the medial trochlear ridge of the femur (ch. 31(1=>0)). Furthermore, they are unambiguously defined by parallel lateral edges of the mandibular spout (ch. 133(1=>0); CI=1/2, RI=3/4), a posterior external opening of mandibular canal that opens laterally on the horizontal ramus (ch. 136(0=>1); non-homoplastic), fused vomerine wings, leaving the overlying ethmoid unexposed (ch. 260(0=>1); CI=1/3, RI=3/5), medial expansion of entotympanic dorsal to floor of basicranium (ch. 292(1=>0); CI=1/4, RI≈0.6), stylomastoid foramen connected to nearby ventral opening of canal for occipital artery by a strong groove (ch. 321(1=>3); CI≈0.4, RI≈0.6), and occipital artery completely enclosed within a canal (ch. 331(1=>3); CI=0.3; RI≈0.7).

According to Gaudin (2004), the clade Megatherioidea includes the Megatheriidae, Nothrotheriidae, and a third family, the Megalonychidae (which comprises the extant two-toed sloth *Choloepus*), along with several Santacrucian taxa whose relationships are not entirely resolved, namely *Schismotherium*, *Pelecyodon*, *Hapalops*, and *Analcimorphus*. Our results yield an unambiguous resolution of the

relationships among these early megatherioids and the three megatherioid families. *Schismotherium* and *Pelecyodon* form a clade that represent the sister-group of all other Megatherioidea, herein called 'clade A.' This clade is not well supported (branch support value of 2), but it is noteworthy that it was also found in one of the MPTs of Gaudin (2004). It is defined by six unambiguous synapomorphies: C1 and c1 slightly depressed ventrally relative to the remaining molariforms (ch. 64(0=>2); CI=1/2, RI=3/5), elongate diastema (ch. 67(0=>1); CI=1/2, RI≈0.8), sphenopalatine foramen situated well anterior and ventral to sphenorbital fissure/optic foramen (ch. 222(1=>0); CI=1/3, RI≈0.7), squamosal with lateral bulge at root of zygoma (ch. 228(0=>1); CI=1/3, RI≈0.7), nuchal crest overhangs occiput posteriorly (ch. 245(0=>1); non-homoplastic), and rugose tympanic external surface (ch. 263 (0=>1); CI=0.5, RI=4/5). *Hapalops* is positioned here as sister-taxon of a clade consisting of *Analcimorphus* and megalonychids, all forming the 'clade B' (Fig. 10). This clade is not well supported either (branch support value of 1), but was also recovered in some of the analyses of Gaudin (2004), depending on the character weighting scheme. The 'clade B' is defined by seven unambiguous synapomorphies: no contact between lunar and unciform (ch. 12(1=>0); CI=1/2, RI=1/2), median position of astragalar process for navicular in distal view (ch. 38(1=>0); non-homoplastic), 18 or more thoracic vertebrae (ch. 51(1=>0); non-homoplastic), elongate and narrow coronoid process of dentary (ch. 108(2=>0); CI= 1/4, RI≈0.6), one posteriorly projecting point on distal portion of descending process of jugal (ch. 215(1=>0); CI=1/4, RI=1/2), median ridge of occiput extends dorsally onto the roof of the skull (ch. 246(0=>1); CI=1/2, RI=1/2), and occipital condyles with distinct neck (ch. 254(0=>1); CI=1/3, RI≈0.8). The Nothrotheriidae are recovered as monophyletic and well supported (branch support value of 9), with eleven unambiguous synapomorphies, among them the presence of a contact between the pterygoid and the

vomer (ch. 193(0=>1); CI=1/2, RI=3/4), the vomer bearing an elongate asymmetrical ventral keel and extending posteriorly into nasopharynx (ch. 261(0=>1), non-homoplastic), and a very large exposure of the vomer, which covers the presphenoid and much of the basisphenoid (ch. 262(0=>1), non-homoplastic).

Discussion and conclusion

Until now, the aquatic sloth *Thalassocnus*, from the Pacific coast of South America, has always been considered member of the extinct family Nothrotheriidae. This was supported by several synapomorphies, but its assignment to this family was never tested in an analysis that included the other megatherian family, the Megatheriidae. Doing so unambiguously indicates that *Thalassocnus* is more closely related to megatheriids than to nothrotheriids. The apomorphies formerly recognized as being shared by *Thalassocnus* and nothrotheriids (De Iuliis *et al.*, 2011) appear rather to be synapomorphies of the more inclusive clade Megatheria. One character that has been used to support the nothrotheriid attribution is worth mentioning as an example - the cross-sectional shape of the ungual process of the ungual phalanx on the second manual digit (McDonald & Muizon, 2002; Muizon *et al.*, 2003; De Iuliis *et al.*, 2011). Whereas nothrotheriids and *Thalassocnus* indeed feature a semi-circular process, the definitive attribution of a second ungual phalanx to *Planops martini* (see text above and Fig. 9) demonstrates that the semi-circular cross-section is in fact a synapomorphy of the Megatheria (with further specializations in megatheriines).

The family Megatheriidae traditionally comprises megatheriines and planopsines [De Iuliis (1994) and references therein; but see Pujos *et al.* (2007)]. The present study advocates the recognition of three megatheriid subfamilies, with the addition of the

monogeneric Thalassocninae, a subfamily formally designated by Muizon *et al.* (2004a). While not formally included in the present phylogenetic analysis, a brief consideration of other megatheriines supports this conclusion. *Megathericulus* is a Friasian and Colloncuran SALMA (Middle Miocene) genus placed in a clade with *Anisodontherium* (Chasicoan SALMA, Late Miocene) that in turn forms the sister-group to all other megatheriines (Pujos *et al.*, 2013). The pattern of postcranial synapomorphies resulting from the present analysis is consistent with this arrangement and with the monophyly of both Thalassocninae and Megatheriinae (the latter encompassing these Miocene taxa not included in the present study). For example, the absence of the entepicondylar foramen (humerus, ch. 4) is consistent with the attribution of *Megathericulus* and *Anisodontherium* to Megatheriinae, since the foramen is also missing in *Megatherium* and *Eremotherium* (De Iuliis, Brandoni, & Scillato-Yané, 2008), but is present in *Thalassocnus* (Fig. 1). Furthermore, the patellar and both condylar surfaces of the distal femur are confluent in *Megathericulus,* whereas the patellar trochlea of the femur (ch. 29) is reduced and confluent with only the lateral condyle in the two later genera, a condition also found in other megatheriines, including the Huayquerian SALMA (Late Miocene) *Pyramiodontherium* (Pujos *et al.*, 2013). The retention of the plesiomorphic condition in *Megathericulus* (as in *Thalassocnus* and *Planops*; Fig. 6) is consistent with its position as a sister-taxon to all other megatheriines.

As a corollary to these taxonomic and phylogenetic patterns, the age of divergence between Thalassocninae and Megatheriinae appears to be Friasian (middle Miocene) or earlier. This early divergence date, combined with the monophyly of both subfamilies, supports the retention of the Thalassocninae, despite the modification of its familial attribution.

One of the results of the present analysis is the confirmation of the stratigraphically congruent phylogenetic relationships among *Thalassocnus* species (in other words, the earliest species is sister-group of all others and so on; Fig. 10). Additionally, several morphoclines oriented from the earliest to the latest species are recognized, and numerous other characters not included in the matrix (because of their non-applicability to other taxa) can also be viewed as morphoclines of the same nature (Amson *et al.*, 2014, 2015a,b,c). Moreover, the autapomorphies of each species except the latest (*T. yaucensis*) are parts of such morphoclines. As a consequence, none of the branches leading to each species except the latest one has an unambiguous length (the lengthening of the Mc II can be recognized as an unambiguous autapomorphy of *T. antiquus*, but a long Mc II is most likely the ancestral state of the genus, because it clearly shortens from the early to the late species). Furthermore, *Thalassocnus* is endemic to the central Pacific coast of South America. As a result, the data are completely congruent with the recognition of Thalassocninae as a distinct anagenetic lineage that evolved in this region. The fossil record of *Thalassocnus* is remarkable in terms of the abundance and completeness of specimens recovered and in the fact that all species derive from a clear stratigraphic sequence in this same geographic area. Of course, the fossil record is never exhaustive, a condition required to formally recognize an anagenetic lineage (Darlu & Tassy, 1993). In spite of this, the record of *Thalassocnus*, which spans over roughly four million years (Muizon *et al.*, 2004a; Ehret *et al.*, 2012), fulfils all the conditions to provide a clear indication of what can be hypothesized as having represented an evolutionary lineage. This hypothesis is supported by the numerous morphoclines concerning the gross morphology of the skull, mandible and dentition (Muizon *et al.*, 2004b), forelimb (Amson *et al.*, 2015a), hind limb (Amson *et al.*, 2015b),

axial postcranium (Amson *et al.*, 2015c), and bone inner microstructure (Amson *et al.*, 2014).

From a functional standpoint, this phylogenetic framework is also consistent with the purported gradual adaptation of *Thalassocnus* to the marine environment, as additional synapomorphies are acquired from the earliest species, *T. antiquus*, to the 'clade Th.1' (*T. natans* and later species), then to the 'clade Th.2' (*T. littoralis* and later species), and then the 'clade Th.3' (*T. carolomartini* and *T. yaucensis*). The latest species (*T. yaucensis*) features all the apomorphies (when characters are known for this species) involved in this adaptation, such as a grazing dentition (Muizon *et al.*, 2004b), shortest metacarpals for powerful digging of subterranean items (most likely rhizomes of seagrasses; Amson *et al.*, 2015a), hind limb features that are the most indicative of a plantigrade posture (likely helpful for bottom-walking; Amson *et al.*, 2015b), and most pachyostotic ribs (helping for buoyancy and trim control; Amson *et al.*, 2014; Amson *et al.*, 2015c). The Thalassocninae hence document with striking detail the evolution of a mammalian clade that adapts to the marine environment.

Acknowledgements

We thank Rodolfo Salas-Gismondi (MUSM), Samuel McLeod and Vanessa Rhue (both LACM), Castor Cartelle (MCL), and Géraldine Veron (MNHN) for allowing one of us (EA) to visit the collections under their care. We are grateful to Greg McDonald (National Park Service) for his insightful discussions about tardigradan phylogeny. The three reviewers are acknowledged for the improvement they brought to the initial manuscript. Finally, Pip Brewer (NHMUK) should receive our warmest thanks for having taken the pictures of the ungual phalanx of the holotype of *Planops martini*. EA was

funded by the CR2P (CNRS, MNHN, UPMC-Paris 06; Sorbonne Universités), the Swiss National Fund grant SNF 31003A_149605 to M. R. Sánchez-Villagra, and the Alexander von Humboldt Foundation.

References

Amson E, Muizon C de, Laurin M, Argot C, Buffrénil V de. **2014**. Gradual adaptation of bone structure to aquatic lifestyle in extinct sloths from Peru. *Proceedings of the Royal Society B* **281**: 20140192.

Amson E, Argot C, McDonald HG, Muizon C de. **2015a**. Osteology and functional morphology of the forelimb of the marine sloth *Thalassocnus* (Mammalia, Tardigrada). *Journal of Mammalian Evolution* **22**: 169–242.

Amson E, Argot C, McDonald HG, Muizon C de. **2015b**. Osteology and functional morphology of the hind limb of the marine sloth *Thalassocnus* (Mammalia, Tardigrada). *Journal of Mammalian Evolution* **22**: 355–419.

Amson E, Argot C, McDonald HG, Muizon C de. **2015c**. Osteology and functional morphology of the axial postcranium of the marine sloth *Thalassocnus* (Mammalia, Tardigrada) with paleobiological implications. *Journal of Mammalian Evolution* **22**: 473–518.

Bargo MS, Vizcaíno SF. **2008**. Paleobiology of Pleistocene ground sloths (Xenarthra, Tardigrada): biomechanics, morphogeometry and ecomorphology applied to the masticatory apparatus. *Ameghiniana* **45**: 175–196.

Bianucci G, Di Celma C, Landini W, Post K, Tinelli C, Muizon C de, Gariboldi K, Malinverno E, Cantalamessa G, Gioncada A, *et al.* 2015. Distribution of fossil marine vertebrates in Cerro Colorado, the type locality of the giant raptorial sperm whale Livyatan melvillei (Miocene, Pisco Formation, Peru). *Journal of Maps*: published online.

Billet G, Germain D, Ruf I, Muizon C de, Hautier L. 2013. The inner ear of *Megatherium* and the evolution of the vestibular system in sloths. *Journal of anatomy* **223**: 557–567.

Canto J, Salas-Gismondi R, Cozzuol MA, Yáñez J. 2008. The aquatic sloth *Thalassocnus* (Mammalia, Xenarthra) from the late Miocene of North-Central Chile: biogeographic and ecological implications. *Journal of Vertebrate Paleontology* **28**: 918–922.

Cartelle C, Fonseca JS. 1983. Contribuição ao melhor conhecimento da pequena preguiça terrícola *Nothrotherium maquinense* (Lund) Lydekker, 1889. *Lundiana* **2**: 127–181.

Cuvier G. 1804. Sur le Megatherium. *Annales du Muséum national d'Histoire naturelle* **5**: 376–400.

Darlu P, Tassy P. 1993. *La reconstruction phylogénétique. Concepts et Méthodes*. Paris: Masson.

De Iuliis G. 1994. Relationships of the Megatheriinae, Nothrotheriinae, and Planopsinae: some skeletal characteristics and their importance for phylogeny. *Journal of Vertebrate Paleontology* **14**: 577–591.

De Iuliis G, Pujos F, Toledo N, Bargo MS, Vizcaíno SF. **2014**. *Eucholoeops* Ameghino, 1887 (Xenarthra, Tardigrada, Megalonychidae) from the Santa Cruz Formation, Argentine Patagonia: implications for the systematics of Santacrucian sloths. *Geodiversitas* **36**: 205–255.

De Iuliis G, Brandoni D, Scillato-Yané GJ. **2008**. New remains of *Megathericulus patagonicus* Ameghino, 1904 (Xenarthra, Megatheriidae): information on primitive features of megatheriines. *Journal of Vertebrate Paleontology* **28**: 181–196.

De Iuliis G, Gaudin TJ, Vicars MJ. **2011**. A new genus and species of nothrotheriid sloth (Xenarthra, Tardigrada, Nothrotheriidae) from the Late Miocene (Huayquerian) of Peru. *Palaeontology* **54**: 171–205.

Ehret DJ, Macfadden BJ, Jones DS, DeVries TJ, Foster DA, Salas-Gismondi R. **2012**. Origin of the white shark *Carcharodon* (Lamniformes: Lamnidae) based on recalibration of the Upper Neogene Pisco Formation of Peru. *Palaeontology* **55**: 1139–1153.

Engelmann GF. **1985**. The phylogeny of the Xenarthra. In: Montgomery GG, ed. The Evolution and Ecology of Armadillos, Sloths, and Vermilinguas. Washington D. C.: Smithsonian Institution Press, 51–64.

Fariña RA, Vizcaíno SF, Bargo MS. **1998**. Body mass estimations in Lujanian (late Pleistocene-early Holocene of South America) mammal megafauna. *Mastozoología Neotropical* **5**: 87–108.

Gaudin TJ. **1995**. The ear region of edentates and the phylogeny of the Tardigrada (Mammalia, Xenarthra). *Journal of Vertebrate Paleontology* **15**: 672–705.

Gaudin TJ. **1999**. The morphology of xenarthrous vertebrae (Mammalia: Xenarthra). *Fieldiana Geology New Series* **41**: 1–38.

Gaudin TJ. **2004**. Phylogenetic relationships among sloths (Mammalia, Xenarthra, Tardigrada): the craniodental evidence. *Zoological Journal of the Linnean Society* **140**: 255–305.

Gazin CL. **1957**. Exploration for the remains of giant ground sloths in Panama. *Smithsonian Institution Annual Report for 1956*: 341–354.

Hoffstetter R. **1952**. Les mammifères pléistocènes de la république de l'Équateur. *Mémoires de la Société Géologique de France* **31**: 375–488.

Hoffstetter R. **1961**. Description d'un squelette de *Planops* (Gravigrade du Miocène de Patagonie). *Mammalia* **25**: 1–96.

Hoffstetter R. **1968**. Un gisement de vertébrés tertiaires à Sacaco (Sud-Pérou), témoin néogène d'une migration de faunes australes au long de la côte occidentale sud-américaine. *Comptes rendus hebdomadaires des séances de l'Académie des sciences. Série D* **267**: 1273–1276.

Leidy J. **1855**. A memoir on the extinct sloth tribe of North America. *Smithsonian Contributions to Knowledge* **7**: 1–68.

Lydekker R. **1894**. Contributions to a knowledge of the fossil vertebrates of Argentina. *Anales del Museo de la Plata, Paleontologia Argentina* **3**: 1–103.

McDonald HG. **1977**. Description of the osteology of the extinct gravigrade edentate *Megalonyx* with observations on its ontogeny, phylogeny, and functional anatomy. Unpublished M. Sci. Thesis, University of Florida.

McDonald HG. **1987**. A systematic review of the Plio-Pleistocene Scelidotherine Ground Sloth (Mammalia, Xenarthra, Mylodontidae). Unpublished D. Phil thesis, University of Florida.

McDonald HG, Muizon C de. **2002**. The cranial anatomy of *Thalassocnus* (Xenarthra, Mammalia), a derived nothrothere from the Neogene of the Pisco Formation (Peru). *Journal of Vertebrate Paleontology* **22**: 349–365.

Muizon C de, McDonald HG, Salas R, Urbina M. **2003**. A new early species of the aquatic sloth *Thalassocnus* (Mammalia, Xenarthra) from the Late Miocene of Peru. *Journal of Vertebrate Paleontology* **23**: 886–894.

Muizon C de, McDonald HG, Salas R, Urbina M. **2004a**. The youngest species of the aquatic sloth *Thalassocnus* and a reassessment of the relationships of the nothrothere sloths (Mammalia: Xenarthra). *Journal of Vertebrate Paleontology* **24**: 287–397.

Muizon C de, McDonald HG, Salas R, Urbina M. **2004b**. The evolution of feeding adaptations of the aquatic sloth *Thalassocnus*. *Journal of Vertebrate Paleontology* **24**: 398–410.

Muizon C de, DeVries TJ. **1985**. Geology and paleontology of late Cenozoic marine deposits in the Sacaco area (Peru). *Geologische Rundschau* **74**: 547–563.

Muizon C de, McDonald HG. **1995**. An aquatic sloth from the Pliocene of Peru. *Nature* **375**: 224–227.

Owen R. **1842**. Description of the skeleton of an extinct gigantic sloth, *Mylodon robustus*, Owen, with observations on the osteology, natural affinities, and probable habits of the megatherioid quadrupeds in general. *Royal College of Surgeons of England London*: 1–176.

Owen R. **1858**. On the Megatherium (*Megatherium americanum*, Cuvier and Blumenbach). Part IV. Bones of the Anterior Extremities. *Philosophical Transactions of the Royal Society of London* **148**: 261–278.

Owen R. **1859**. On the Megatherium (*Megatherium americanum*, Cuvier and Blumenbach). Part V. Bones of the Posterior Extremities. *Philosophical Transactions of the Royal Society of* **149**: 809–829.

Owen R. **1861**. Memoir on the Megatherium, or giant ground-sloth of America (*Megatherium americanum*, Cuvier). Philosophical Transactions of the Royal Society of London. London: Williams and Norgate, 84, 27 pl.

Patterson B, Segall W, Turnbull WD, Gaudin TJ. **1992**. The ear region in xenarthrans (= Edentata: Mammalia) Part II. Pilosa (Sloths, Anteaters), palaeanodonts, and a miscellany. *Fieldiana Geology New Series* **24**: 1–79.

Paula Couto C de. **1974**. The manus of *Nothrotheriops shastense* (Sinclair, 1905). *Anais do XXVIII Congresso Brasileiro de Geologia* **2**: 165–176.

Pujos F. **2002**. Contribution à la connaissance des tardigrades (Mammalia: Xenarthra) du Pléistocène péruvien: systématique, phylogénie, anatomie fonctionnelle et extinction.

Pujos F, De Iuliis G, Argot C, Werdelin L. **2007**. A peculiar climbing Megalonychidae from the Pleistocene of Peru and its implication for sloth history. *Zoological Journal of the Linnean Society* **149**: 179–235.

Pujos F, Salas R, Baby G, Baby P, Goillot C, Tejada J, Antoine PO. **2013**. Implication of the presence of *Megathericulus* (Xenarthra: Tardigrada: Megatheriidae) in the Laventan of Peruvian Amazonia. *Journal of Systematic Palaeontology* **11**: 973–991.

Pyenson ND, Gutstein CS, Parham JF, Little H, Metallo A, Roux P Le, Carren C, Rossi V, Valenzuela-Toro AM, Velez-Juarbe J, *et al.* 2014. Repeated mass strandings of Miocene marine mammals from Atacama Region of Chile point to sudden death at sea. *Proceedings of the Royal Society B* **281**: 20133316.

Scott WB. **1903-1904**. Mammalia of the Santa Cruz beds. *Reports of the Princeton University Expeditions to Patagonia* **5**: 1–490.

Stock C. **1925**. Cenozoic gravigrade edentates of western North America, with special reference to the Pleistocene Megalonychinae and Mylodontidae of Rancho La Brea. *Carnegie Institution of Washington Publications* **331**: 1–206.

Swofford DL. **2002**. PAUP: phylogenetic analysis using parsimony. Version 4.0b10.

Tito G. **2008**. New remains of *Eremotherium laurillardi* (Lund, 1842) (Megatheriidae, Xenarthra) from the coastal region of Ecuador. *Journal of South American Earth Sciences* **26**: 424–434.

Toledo N, Bargo MS, Vizcaíno SF. **2015**. Muscular reconstruction and functional morphology of the hind limb of Santacrucian (early Miocene) sloths (Xenarthra, Folivora) of Patagonia. *Anatomical Record* **298**: 842–864.

Figure Legends

Figure 1. Anterior view of the distal epiphysis of the right humerus among megatherioid sloths. A, *Hapalops longiceps* (from Scott, 1903-1904); B, *Nothrotheriops shastensis*; C, *Thalassocnus littoralis*; D, *Megatherium americanum* (from Owen, 1858). Not to scale.

Figure 2. Anterior view of the distal epiphysis of the right radius among megatherioid sloths. A, *Hapalops longiceps* (from Scott, 1903-1904); B, *Nothrotheriops shastensis*; C, *Thalassocnus littoralis*; D, *Megatherium americanum*. Not to scale.

Figure 3. Dorsal view of the articulated left manus among Megatheria. A, *Thalassocnus carolomartini*; B, *Mionothropus cartellei* (from De Iuliis *et al.*, 2011); C, *Megatherium americanum* (from Owen, 1858). Not to scale. Abbreviations: D., digit; Mc, metacarpal; MCC, metacarpal-carpal complex; ph., phalanx.

Figure 4. Dorsal view of the left lunar among *Nothrotheriops* and *Thalassocnus*. A, *Nothrotheriops shastensis* (LACM 156468); B, *Thalassocnus antiquus* (MUSM 228); C, *Thalassocnus natans* (MNHN.F.SAS734); D, *Thalassocnus carolomartini* (MUSM 1995). Abbreviation: f., facet.

Figure 5. Posterior view of the right femur among megatherioid sloths. A, *Hapalops* sp.; B, *Planops martini*; C, *Thalassocnus littoralis*; D, *Megatherium americanum*. Not to scale. Abbreviations: fov. cap., fovea capitis; great. troch., greater trochanter; lat. cond., lateral condyle; lat. epic., lateral epicondyle; less. troch., lesser trochanter; med. cond., medial condyle; med. epic., medial epicondyle; 3rd troch., third trochanter.

Figure 6. Distal view of the right femur among Megatheria. A, *Thalassocnus antiquus* (MUSM 228; with interpretative drawing on the right side); B, *Thalassocnus natans* (MNHN.F.SAS734); C, *Thalassocnus littoralis* (MUSM 223); D, *Thalassocnus carolomartini* (MNHN.F.SAO201); E, *Thalassocnus yaucensis* (MUSM 434); F, *Planops martini*, G, *Nothrotheriops shastensis*; H, *Megatherium americanum*. Abbreviations: lat. cond., lateral condyle; lat. epic., lateral epicondyle; lateral trochlear ridge, lat. troch. ridge; LTR, anteroposterior depth at lateral trochlear ridge; med. cruc. lig. notch, notch for medial cruciate ligament; med. cond., medial condyle; med. epic., medial epicondyle; med. troch. ridge, medial trochlear ridge; MTR, anteroposterior depth of medial trochlear ridge anterior to lateral one; pat. troch., patellar trochlea.

Figure 7. Plantar view of the left calcaneum among Megatheria. A, *Nothrotheriops shastensis*; B, *Planops martini*; C, *Thalassocnus littoralis*; D, *Megatherium americanum*. Not to scale.

Figure 8. Dorsal view of the articulated left pes among Megatheria. A, *Nothrotheriops shastensis*, B, *Thalassocnus natans*; C, *Megatherium americanum*. Not to scale. Abbreviations: D., digit; MEC, mesocuneiform-entocuneiform complex; Mt, metatarsal; ph., phalanx.

Figure 9. Ungual phalanx of the second manual digit of *Planops martini* (NHMUK PV M9217f, part of the holotype lot; Hoffstetter, 1961). A, Dorsal view; B, palmar view; C, lateral view; D, proximal view.

Figure 10. Phylogeny of megatherioid sloths. The PAUP heuristic search (Swofford, 2002) resulted in a single most parsimonious tree (CI = 0.47, RI = 0.62). The numbers at the nodes are the branch support values. Abbreviations: Moi., Megatherioidea; Myc., Megalonychidae.

Tables

Table 1. Data matrix of the postcranial characters and cranial characters of special relevance to *Thalassocnus*.

Character number	1	2	3	4	5	6	7	8	9	10	11	12	13	14	15	16	17	18	19	20	21	22	23	24	25	26	27	28	29	30	31	32	33	34	35	36	37	38	39	40	41	42	43	44	45	46	47	48	49	50	51	52	53	54	55	56	57	58	59	60	61
Bradypus	0	0	1	1	0	0	-	0	0	0	1	1	0	0	0	-	1	2	2	1	0	1	0	1	0	1	-	-	a	0	1	0	1	1	0	-	2	1	1	0	0	0	2	1	-	-	-	-	-	0	a	-	-	?	0	0	-	0	0	0	0
Nematherium	1	0	0	0	0	0	?	0	?	?	?	?	?	?	?	?	?	?	?	?	?	?	?	?	?	?	?	?	?	?	?	?	?	?	1	?	?	?	?	0	?	?	?	?	?	?	?	?	?	?	?	?	?	?	?	?	?	?	?	?	?
Glossotherium	1	1	0	1	0	0	0	0	1	1	1	1	0	0	0	0	-	2	0	2	1	0	0	1	?	0	1	2	0	0	0	0	0	0	2	1	1	1	0	1	-	1	2	0	2	1	1	0	1	1	1	0	0	?	0	0	0	1	0	1	-
Catonyx	1	0	0	1	0	0	0	0	0	0	1	1	0	0	0	0	0	0	0	2	1	0	-	1	0	0	1	2	0	0	0	0	0	0	2	1	2	1	0	0	1	1	2	1	2	0	1	0	0	1	?	0	?	?	0	0	0	1	?	0	0
Hapalops	0	0	0	0	0	0	-	0	0	0	0	0	0	0	0	?	0	-	0	?	0	0	0	0	0	0	0	0	0	0	1	0	0	0	1	0	0	0	1	0	0	0	1	0	2	0	0	0	0	0	0	0	?	0	0	0	0	0	0	0	0
Megalonyx	1	0	0	0	0	0	-	0	1	?	1	0	0	0	1	0	0	?	0	?	0	0	0	1	?	0	0	0	1	0	1	0	0	0	0	-	0	0	0	0	0	0	0	a	2	0	1	0	0	0	0	0	?	?	0	0	-	0	0	0	0
Eucholoeops	0	0	0	0	0	0	?	?	?	?	?	?	?	?	?	?	?	1	0	1	?	0	?	?	?	0	?	0	1	?	1	?	0	?	?	?	?	?	?	?	?	?	?	?	1	0	0	0	0	0	?	?	?	?	0	0	?	0	?	0	0
Planops	0	0	1	0	0	1	0	1	?	?	?	?	?	?	?	?	?	?	?	?	1	?	?	?	0	0	0	0	0	1	0	?	0	0	2	0	1	1	1	0	1	0	?	?	?	?	?	?	?	?	?	?	?	?	?	?	?	0	0	?	?
Eremotherium laurillardi	1	0	1	1	0	1	-	1	1	0	1	1	1	0	0	-	-	2	2	-	-	1	1	1	?	0	1	2	2	0	-	?	?	1	2	1	1	1	1	1	1	0	2	1	?	?	2	0	1	1	1	?	?	?	0	0	0	0	0	0	0
Megatherium americanum	2	0	1	1	0	1	-	1	0	0	1	1	1	0	0	1	1	2	2	1	2	1	0	1	0	0	1	2	2	0	-	0	0	1	2	1	1	1	1	1	1	0	2	1	2	1	2	0	1	1	1	0	0	?	2	1	0	0	0	0	0
Mionothropus	0	?	0	0	0	1	0	0	0	0	1	0	1	1	0	0	0	-	0	0	1	0	0	1	?	0	0	0	1	0	0	?	?	?	?	?	?	?	?	?	?	?	?	?	?	?	?	?	?	?	?	?	?	?	0	0	0	0	0	?	?
Pronothrotherium	?	?	?	?	?	1	?	?	?	?	?	?	?	?	?	?	?	?	?	?	1	?	?	?	?	?	?	?	?	?	?	?	?	?	?	?	?	?	?	?	?	?	?	?	?	?	?	?	?	?	?	?	?	?	?	?	?	0	0	?	?
Nothrotherium	0	0	0	0	0	1	-	0	1	0	1	1	0	0	0	0	0	0	0	0	1	0	0	1	0	0	0	0	1	0	1	0	0	0	1	0	0	1	1	0	0	0	1	1	1	0	1	0	0	2	1	0	1	0	0	0	0	0	0	0	0
Nothrotheriops	0	0	0	0	0	1	-	0	1	0	1	1	0	0	0	0	0	0	0	1	1	0	0	1	0	0	0	3	1	0	0	0	0	0	1	0	0	1	1	0	0	0	1	1	1	0	1	0	0	2	1	1	1	0	0	0	0	0	0	0	0
T. antiquus	1	0	1	0	0	1	?	1	0	0	0	1	0	0	0	1	1	1	1	0	1	1	1	1	1	1	1	1	0	0	0	1	?	1	2	1	1	1	1	1	1	0	2	?	0	1	1	1	1	1	?	1	?	0	1	1	0	1	0	0	1
T. natans	1	1	1	0	1	1	0	1	0	1	0	1	0	0	0	1	1	?	1	1	1	1	1	1	?	1	1	1	0	0	1	1	1	1	2	1	1	1	1	1	1	0	2	1	0	1	1	1	1	1	1	1	0	1	1	1	0	1	0	0	1
T. littoralis	1	1	1	0	2	1	1	1	0	1	1	1	0	0	1	1	1	1	1	1	1	1	1	1	1	1	1	1	0	1	1	1	1	1	2	1	1	1	1	1	1	0	2	1	1	1	1	1	1	1	1	2	0	2	2	1	1	1	1	1	1
T. carolomartini	1	1	1	0	3	1	2	1	0	1	1	1	0	1	1	1	1	1	1	1	1	1	1	1	1	1	1	1	0	1	1	1	1	1	2	1	1	1	1	1	1	0	2	1	1	1	1	1	1	1	?	3	?	2	2	1	1	1	2	1	1
T. yaucenis	1	1	1	0	3	1	2	1	0	?	1	1	0	1	2	1	1	1	1	2	1	0	1	1	?	1	1	1	0	1	1	1	?	1	1	0	1	1	1	1	1	0	?	1	2	1	1	1	1	1	1	3	0	?	2	1	1	0	2	1	1
Analcimorphus	?	?	?	?	?	?	?	?	?	?	?	?	?	?	?	?	?	?	?	?	?	?	?	?	?	0	0	0	?	?	1	?	0	0	0	?	?	?	?	?	?	?	0	0	2	?	0	0	0	0	?	?	?	?	?	?	?	0	0	?	?
Schismotherium	?	?	0	0	?	?	?	?	?	?	?	?	0	0	0	?	?	?	0	?	?	0	?	0	?	?	-	?	?	?	?	?	?	?	?	?	?	?	?	0	0	?	?	?	?	?	?	?	?	?	?	?	?	?	?	?	?	0	?	0	0
Pelecyodon	0	0	0	0	?	?	?	?	?	?	?	?	?	?	?	?	?	?	?	?	?	?	?	?	?	?	?	0	0	?	1	?	0	0	?	?	?	?	?	0	?	?	?	0	2	?	0	0	1	0	?	?	?	?	?	?	?	0	?	0	0

Footnotes: Abbreviation: a, 0/1.

Table 2. Source of coding for postcranial characters.

Terminal taxa	Specimens observed	Literature consulted
Bradypus	MNHN.1970-96; MNHN.1996-591; MNHN.1996-590	-
Nematherium	FMNH P13129; FMNH P13131; FMNH P13258; FMNH XPMPU15324;	(Scott, 1903-1904)
Glossotherium	MNHN.F.TAR767; MNHN.F.PAM141, 128	(Owen, 1842; Lydekker, 1894)
Catonyx	MCL 22394; MCL 22396; MCL 22397; MCL 2247; MCL 4265	(McDonald, 1987)
Hapalops	Batch number MNHN.F.1902-6.	(Scott, 1903-1904)
Megalonyx	-	(Leidy, 1855; McDonald, 1977)
Eucholoeops	-	(Scott, 1903-1904; De Iuliis *et al.*, 2014)
Planops	NHMUK PV M9217f (photographs); NHMUK PV M9207-92013, 9215b, 9215c, 9215e (casts).	(Hoffstetter, 1961)
Eremotherium laurillardi	-	(Hoffstetter, 1952; Gazin, 1957; Tito, 2008)
Megatherium americanum	MNHN.1871-3 (mounted specimen of the MNHN)	(Owen, 1858, 1859, 1861)
Mionothropus	LACM 4609/117533	(De Iuliis *et al.*, 2011)
Pronothrotherium	-	(De Iuliis *et al.*, 2011)
Nothrotherium	MCL 1020	(Cartelle & Fonseca, 1983)
Nothrotheriops	Various numbered and unnumbered specimens of the LACM collections	(Stock, 1925)
Thalassocnus	See lists of specimen of Amson *et al.* (2015a,b,c)	-
Analcimorphus	-	(Scott, 1903-1904)
Schismotherium	-	(Scott, 1903-1904)
Pelecyodon	-	(Scott, 1903-1904)

Appendices

Appendix 1. Nexus file containing the data matrix.

Appendix 1. Correspondence between the numbering systems used in the present analysis and those of Gaudin (1995, 2004).

Appendix 3. Tables displaying the calculated ratios for the characters that include numerical values.

Appendix 4. Table of linkages provided by PAUP.

Appendix 5. List of apomorphies (under DELTRAN optimization) provided by PAUP.

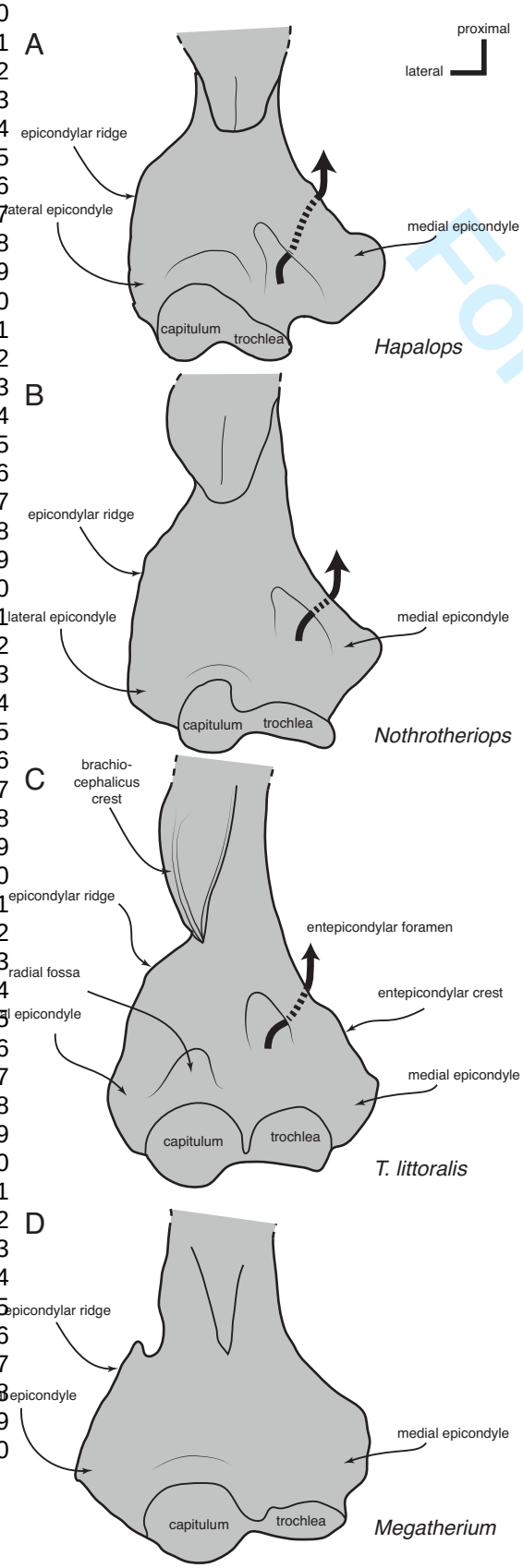

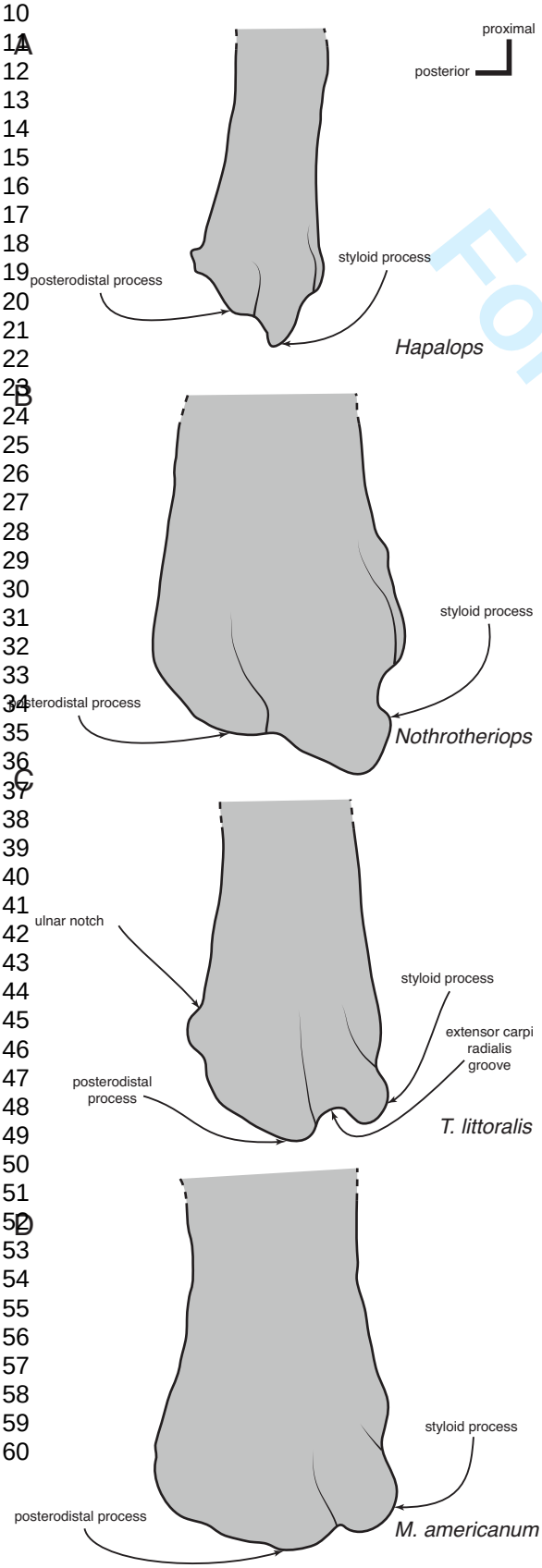

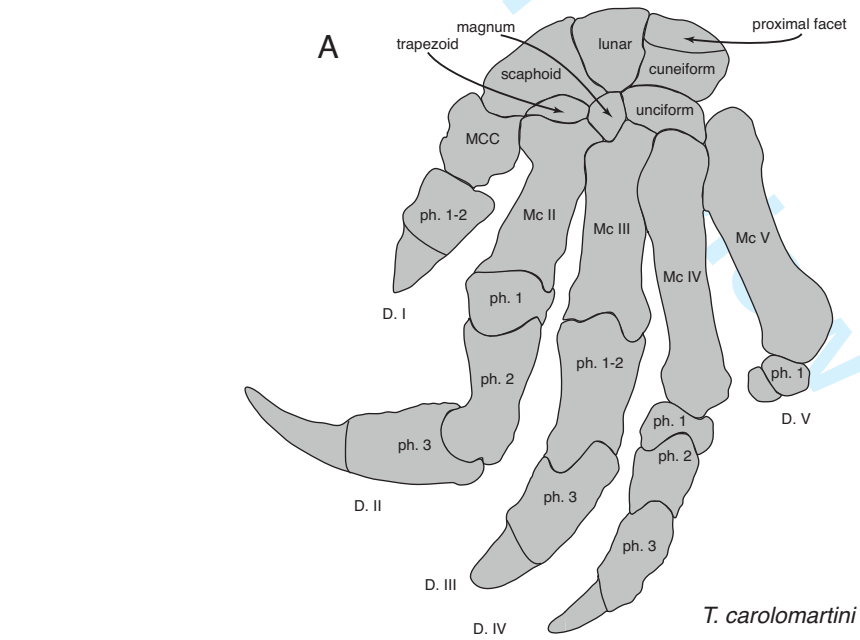

T. carolomartini

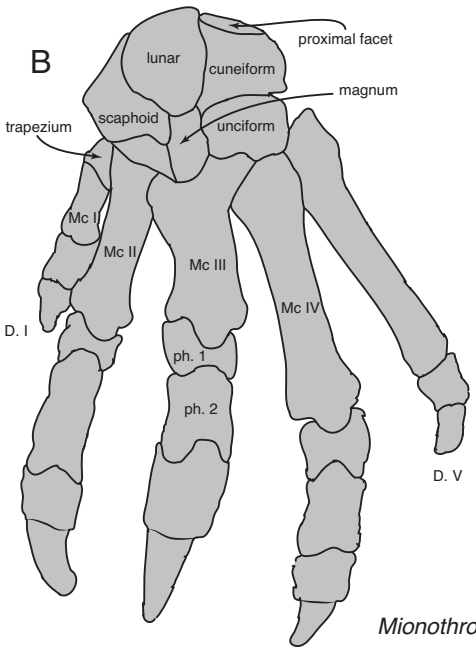

Mionothropus

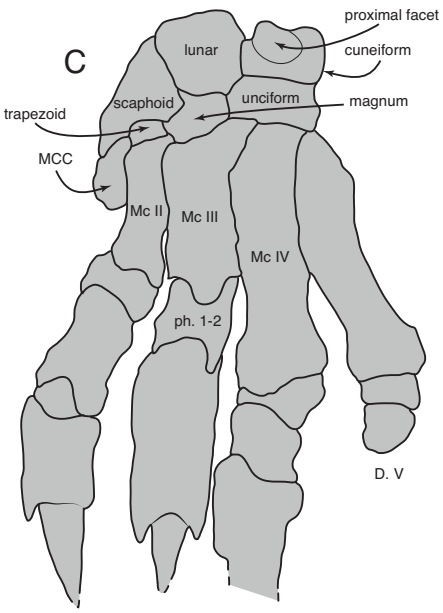

M. americanum

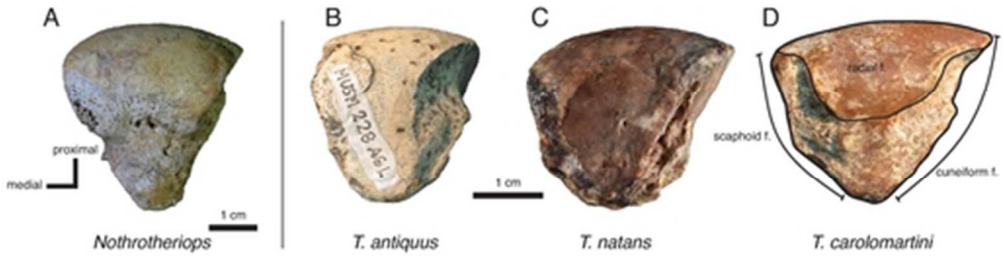

Figure 4. Dorsal view of the left lunar. A, Nothrotheriops (LACM 156468); B, Thalassocnus antiquus (MUSM 228); C, Thalassocnus natans (MNHN.F.SAS734); D, T. carolomartini (MUSM 1995). Abbreviation: f., facet.
43x11mm (300 x 300 DPI)

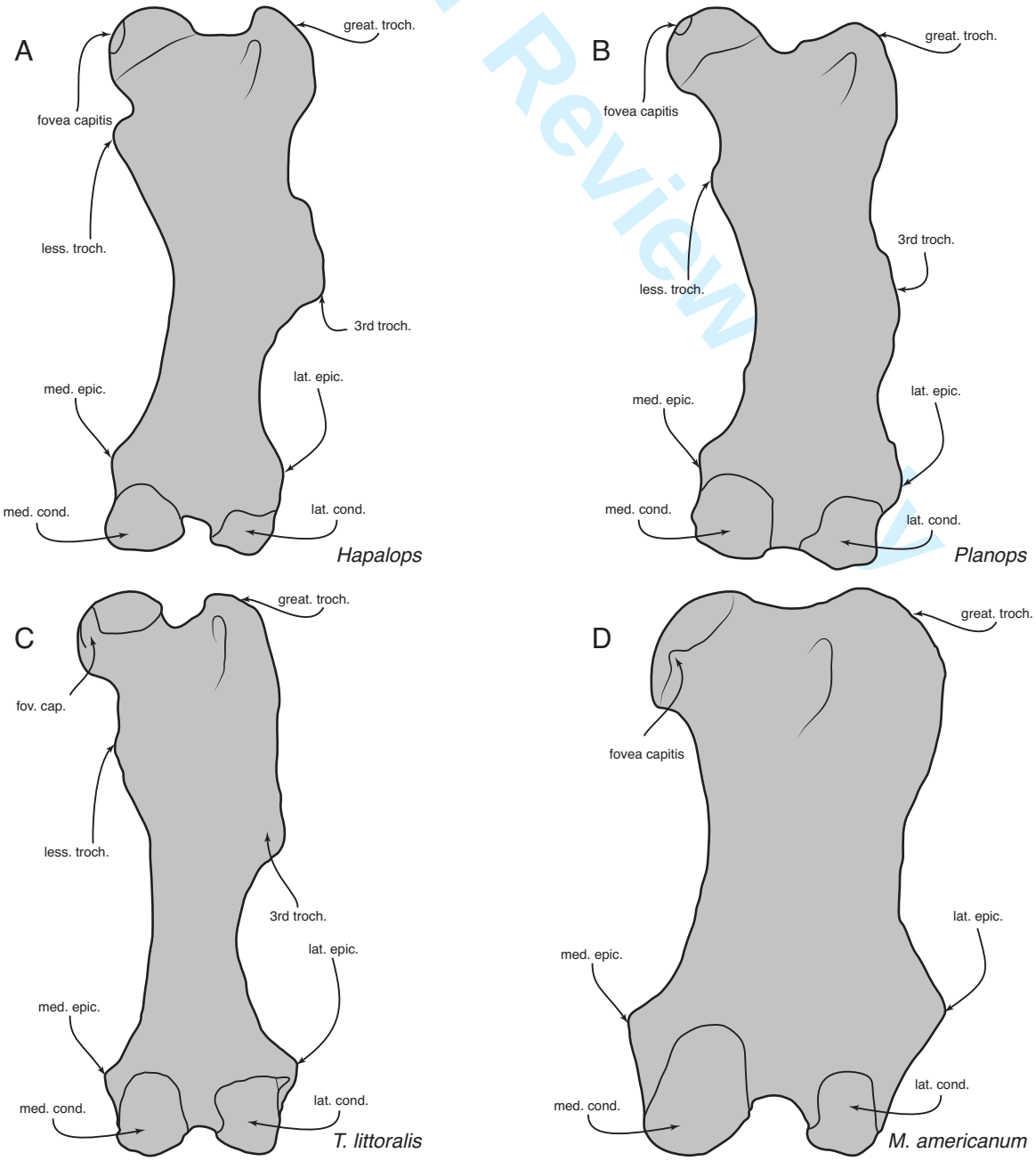

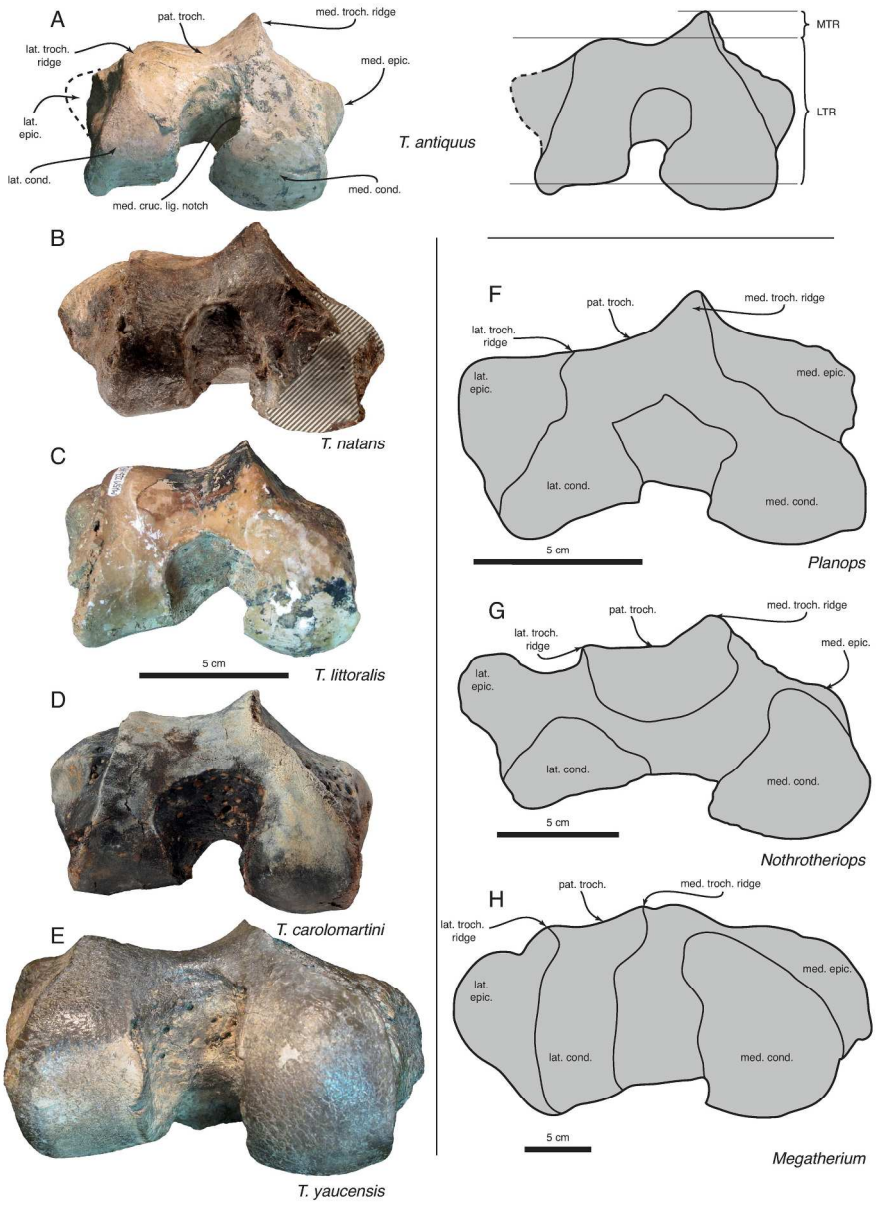

Figure 6. Distal view of the right femur. A, Thalassocnus antiquus (MUSM 228; with interpretative drawing on the right side); B, Thalassocnus natans (MNHN.F.SAS734); C, Thalassocnus littoralis (MUSM 223); D, Thalassocnus carolomartini (MNHN.F.SAO201); E, Thalassocnus yaucensis (MUSM 434); F, Planops, G, Nothrotheriops; H, Megatherium americanum. Abbreviations: lat. cond., lateral condyle; lat. epic., lateral epicondyle; lateral trochlear ridge, lat. troch. ridge; LTR, anteroposterior depth at lateral trochlear ridge; med. cruc. lig. notch, notch for medial cruciate ligament; med. cond., medial condyle; med. epic., medial epicondyle; med. troch. ridge, medial trochlear ridge; MTR, anteroposterior depth of medial trochlear ridge anterior to lateral one; pat. troch., patellar trochlea.
224x301mm (300 x 300 DPI)